

PAPER

Nondestructive technique for estimating crack positions in a concrete structure by subtraction of the surface-wave component

Takeshi Murakami*, Toyota Fujioka, Yoshifumi Nagata and Masato Abe

Faculty of Engineering, Iwate University, Ueda 4-3-5, Morioka, 020-8551 Japan

(Received 25 September 2006, Accepted for publication 6 February 2007)

Abstract: In this paper, we describe a method for estimating a crack position in a concrete structure using several accelerometers. An array of accelerometers is attached to the concrete structure and an impact is made on the concrete surface using a small impulse hammer. A reflection wave is generated from the crack position if a crack exists. Conventional methods for estimating the reflection point might seem to be useful for the detection of cracks. Because the concrete structure is elastic, however, it has three wave-propagation modes: the surface-wave mode, the primary-wave mode, and the secondary-wave mode. We cannot estimate the position using conventional methods because the necessary primary-wave mode is weaker than the surface-wave mode. To estimate the crack position precisely, we have already proposed two methods for eliminating the surface-wave and side-wall reflections. However, elimination using those methods was insufficient because they sometimes indicated a peak at a position where no crack existed. Therefore, in this paper, we propose a new method for estimating the surface wave more precisely to suppress such peaks. Some experiments were carried out, yielding better results.

Keywords: Nondestructive measurement, Elastic wave, Multiple sensors, Beamforming

PACS number: 43.40.Le, 43.60.Gk, 43.60.Rw [doi:10.1250/ast.28.310]

1. INTRODUCTION

Structural-health monitoring techniques have been developed extensively since the 1995 Kobe earthquake to detect (1) the presence or absence of cracks, (2) crack positions, and (3) crack sizes in large structures such as tunnels, dams, and buildings. For such applications, an approximate evaluation of the position and crack size is sufficient. Nondestructive methods of finding a crack in a concrete structure are classifiable into three categories: (1) methods using X-rays [1], (2) methods using IR thermography [2], and (3) methods using a vibration signal [3-6]. The first method cannot locate small cracks such as those in a thin plate; the second requires that the measuring point is viewed directly. Moreover, neither is useful for finding cracks deep within a structure. Therefore, the third type of method has been widely investigated. The concrete structure investigated in our project is very large (larger than 1 m). For this reason, we use a low-frequency vibration signal instead of an ultrasonic one. In conventional methods, low-frequency vibration signals are driven into the concrete structure by an impact force to estimate

the resonant frequency of the concrete structure. Thereby, the position of the crack is estimated [3,4]. However, this method only works well for some cases in which: (1) the crack resembles a sheet and the sheet is parallel to the structure surface (a standing wave is generated in this case), or where (2) the crack is large so that it causes a shift in the resonant frequency. We have already proposed several methods for estimating the position of a sheetlike crack in a concrete structure using several accelerometers. Using such methods, the position of the first reflection wave from the crack caused by the impact force is used to find the crack position instead of the resonant frequency. The positions of cracks can be estimated by this method when the concrete structure has more than one crack [6], but it is very difficult to estimate the locations using the other conventional methods. Furthermore, this method works well even when the sheetlike crack is slanted to the surface of the concrete structure.

In our method, an array of accelerometers is attached to the concrete structure; then, an impact is driven into the concrete by hitting the surface with a small hammer. The hammer produces low-frequency components of less than 10 kHz, which do not decrease in power during propagation as higher-frequency components do. Therefore, reflections

*e-mail: mtakeshi@iwate-u.ac.jp

from a crack are detectable, even if the crack is located deep within the structure. Because low-frequency components are less than 10 kHz in our method, the crack size, which is detectable, might be the same as the wavelength. However, some experiments have shown that a 1-cm-thick sheetlike crack is detectable using our method. Because the concrete structure is elastic, three wave-propagation modes exist: the surface-wave mode, the primary-wave mode, and the secondary-wave mode. The necessary primary-wave mode is weak compared with the surface-wave mode. This problem is negligible in the conventional method [3], which estimates the resonant frequency, but it is a significant obstacle in our method. To estimate the crack position precisely, we have already proposed two methods. One is a method that eliminates only the first-arriving surface wave [5]; the other is a method that eliminates the surface wave and reflections from side walls [6]. This process works well because (1) the distance between the point of impact and the accelerometer is sufficiently longer than the thickness of the concrete structure, and (2) the impulse response caused by the reflections from the side wall is nearly identical for each accelerometer. To reiterate, if the concrete structure is sufficiently small that the reflections from side walls overlap with the surface wave, this method does not work well. In this case, it is difficult to detect a crack. Therefore, a new method that eliminates the surface-wave precisely is anticipated.

In this paper, we propose a new method for detecting a crack more accurately by estimating the surface wave more precisely. Our experiments have revealed that the crack position is more clearly detectable by our new method.

2. PRECISE ESTIMATION OF A SURFACE WAVE

An impact with a hammer generates a surface wave, a primary wave, and a secondary wave. The surface-wave power decreases in proportion to the propagation distance, whereas those of the primary wave and the secondary wave decrease in proportion to the square of the propagation distance. Therefore, the surface wave becomes dominant at positions far from the impact point. On the other hand, the primary wave and the secondary wave are dominant for reflections from a crack. The primary wave is known to be particularly dominant for the reflection from a crack directly underneath the point of impact.

2.1. Accelerometer Output Attributable to the Impact of an Impulse Hammer

We assume that an elastic structure has a crack, as shown in Fig. 1. Several accelerometers are attached to the stress-free surface of the structure. A location almost at the center of the accelerometer array is struck with a small impulse hammer. Figure 2 shows the impact force and its

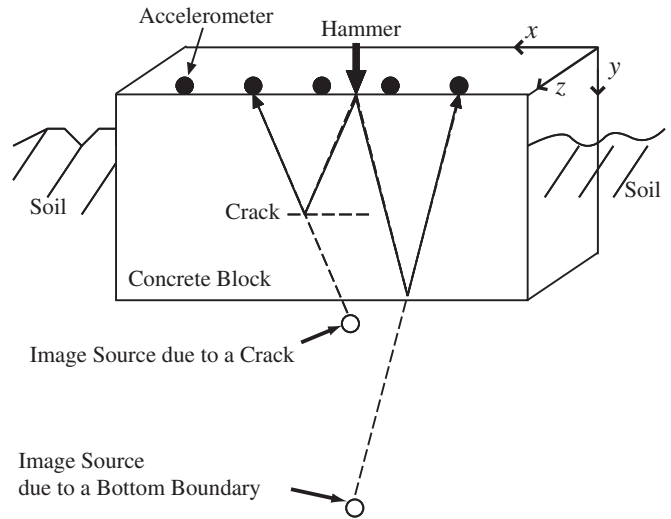


Fig. 1 Elastic structure buried in the soil.

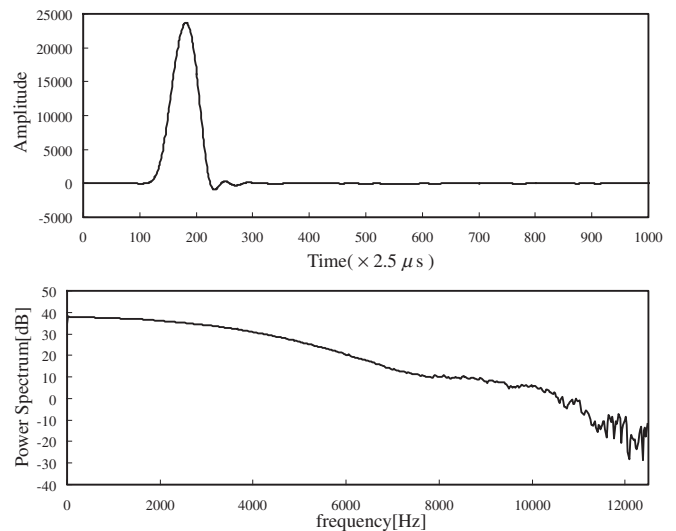


Fig. 2 Impact force $f(n)$ and its power spectrum produced using a small impulse hammer.

power spectrum.

Because the waveform of the impact force shows only a single peak, we inferred that the accelerometer output also shows only a single peak. Accordingly, some experiments were carried out on the wall of a large dam as a concrete structure that might have no cracks and no reflections. Figure 3 shows an example of the response to an impact with a small impulse hammer. Figure 3 shows that the accelerometer output is not expressed by a single peak, perhaps because of (1) the accelerometer setting and (2) the frequency characteristics of the accelerometer and the amplifier. In all experimental cases, the accelerometer outputs resemble that shown in Fig. 3.

Extraction of the precise surface wave should be performed by deconvolution. However, a stable inverse

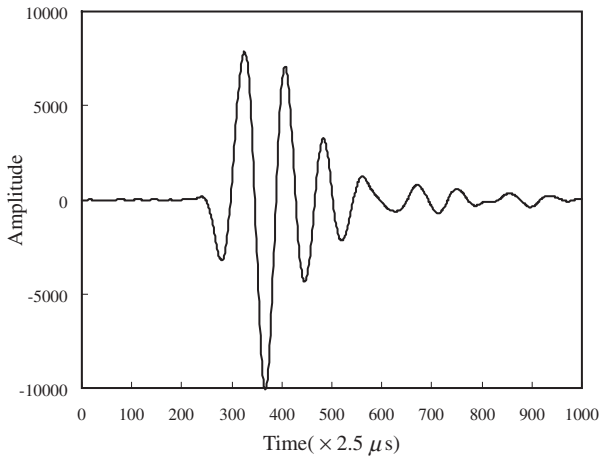


Fig. 3 Accelerometer output elicited by an impact to a large dam wall using a small impulse hammer.

filter cannot be obtained using the deconvolution technique because the transfer function from the impact force to the accelerometer output has zeros. For this reason, the extraction is performed as follows. We infer from Fig. 3 that the original output $u_m(n)$ of the m th accelerometer is modeled approximately by an exponentially decaying sinusoidal wave in the interval where the impact force is absent. An impulse response $h_m(n)$ expressed using the following equation is therefore introduced for the m th accelerometer:

$$h_m(n) = \alpha \exp(-\beta_m n) \cos(2\pi\gamma_m n + \theta_m), \quad (1)$$

where n is the discrete time, where the time is expressed as $t = n\Delta T$ and ΔT is the sampling period.

The estimated surface wave $u'_m(n)$ is expressed as

$$u'_m(n) = \sum_{p=0}^{N-1} f(n-p)h_m(p), \quad (2)$$

where $f(n)$ is the impulse hammer output, N is the length of the impulse response $h_m(n)$, and N is set to 1,024 points (2.56 ms) in the experiment.

Here, the original output $u_m(n)$ of the m th accelerometer passed through a charge amplifier in the experiment, and the effect of the charge amplifier should be compensated. Because the charge amplifier was a type of a high-pass filter, the difference $f'(n) = f(n) - f(n-1)$ of the impulse hammer output (impact force) was used as the simplest high-pass filter instead of the original output $f(n)$ of the impulse hammer. The estimated surface wave $u''_m(n)$ using $f'(n)$ instead of $f(n)$ is expressed as

$$u''_m(n) = \sum_{p=0}^{N-1} f'(n-p)h_m(p). \quad (3)$$

The four parameters α_m , β_m , γ_m , and θ_m are determined to minimize the following mean-square error.

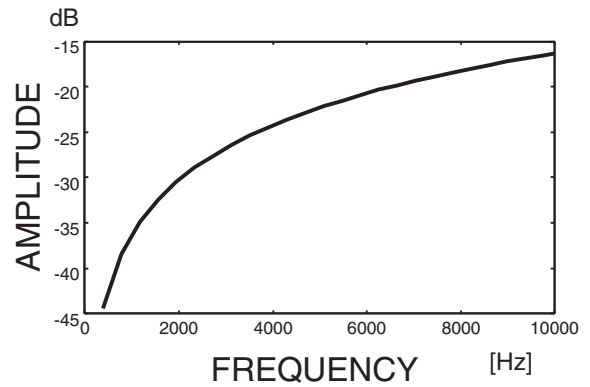


Fig. 4 Transfer function of the high-pass filter realized by the difference $f'(n) = f(n) - f(n-1)$.

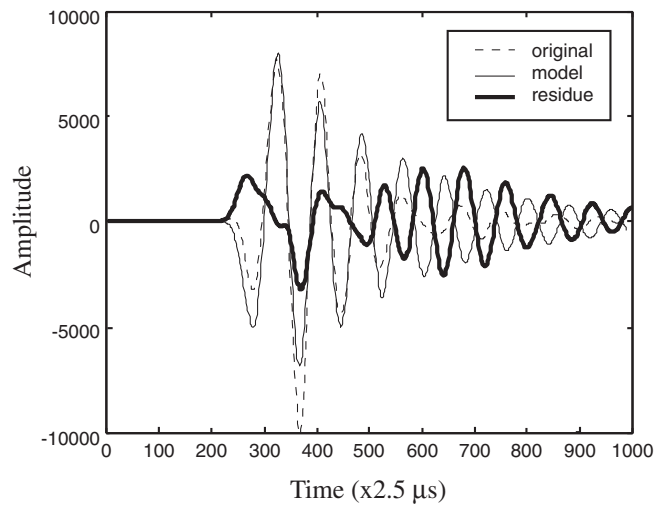


Fig. 5 Original output $u_m(n)$, the modeled output $u'_m(n)$ using $f(n)$ and their residue for the case shown in Fig. 3.

$$E = \begin{cases} \sum_n |u'_m(n) - u_m(n)|^2, & \text{for } f(n) \\ \sum_n |u''_m(n) - u_m(n)|^2, & \text{for } f'(n) \end{cases} \quad (4)$$

For this equation, the duration of summation \sum_n is chosen so that only the surface wave appears in the duration. The method of determining the duration is explained in Sect. 2.2.

Figure 4 shows the transfer function of the high-pass filter realized by the difference $f'(n) = f(n) - f(n-1)$.

Figure 5 shows the original waveform $u_m(n)$, the modeled output of the surface wave $u'_m(n)$, and their residue $\langle u_m(n) - u'_m(n) \rangle$ when E reaches a minimum. Figure 6 shows the original waveform $u_m(n)$, the modeled output of the surface wave $u''_m(n)$, and their residue $\langle u_m(n) - u''_m(n) \rangle$ when E reaches a minimum. Comparison of Fig. 5 with Fig. 6 clarifies that $u''_m(n)$ using $f'(n)$ is a

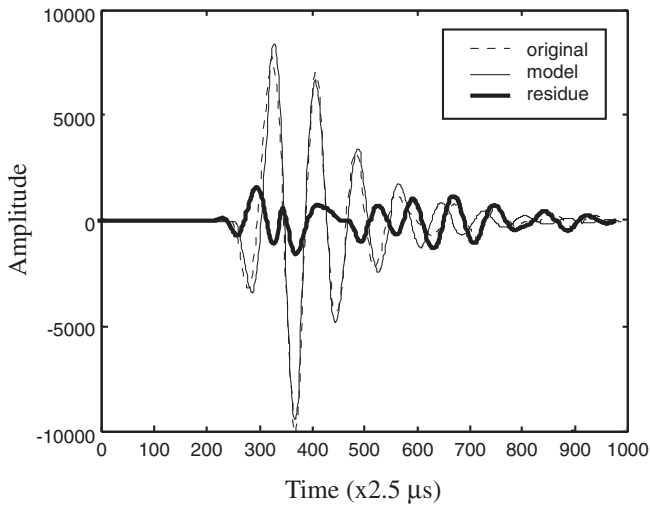


Fig. 6 Original output $u_m(n)$, the modeled output $u'_m(n)$ using $f'(n)$ and their residue for the case shown in Fig. 3.

better model of the surface wave than $u'_m(n)$ using $f(n)$. (The error E using the original force $f(n)$ is 3.1 times larger than that using the difference $f'(n)$.) The difference $f'(n)$ might not be the best high-pass filter, but it is better to use the difference $f'(n)$ than to use the original force $f(n)$.

The residues in Figs. 5 and 6 might be attributable to (1) the primary and the secondary waves, which are not taken into account here, and (2) the estimation error of the surface wave. The power of the residue in Fig. 6 is smaller than that of the original wave by about 12 dB. On the other hand, the difference between the peak value caused by the reflection wave from the opposite wall or crack (the desired signal) and that from the side wall (interference or noise) is about 5 dB, as described in Sect. 4. That is, the signal-to-noise ratio (SNR) is 5 dB. The estimation accuracy (12 dB) of the surface wave is sufficient compared with the SNR (5 dB).

2.2. Estimation of a Surface Wave for a Real Concrete Structure

The impulse response of an accelerometer and the attached amplifier used in this section are the same as those used in Sect. 2.1, the extraction of the surface wave can be executed similarly. The method explained in Sect. 2.1 was applied to the concrete species shown in Fig. 7.

Figures 8 and 9 respectively depict the original accelerometer output, the estimated surface wave, and the residue for concrete species (c) by the previous method [6] and the new method proposed here.

The duration for which the error E is calculated is determined as follows:

- (1) The starting point of the duration is set at the initial rising point of the first peak.

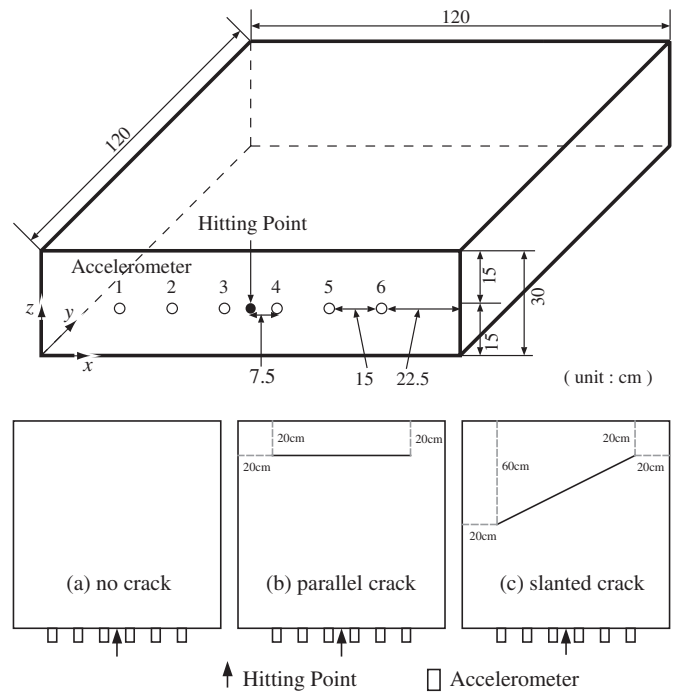


Fig. 7 Three concrete species used in the experiments: (a) no crack, (b) parallel crack, and (c) slanted crack.

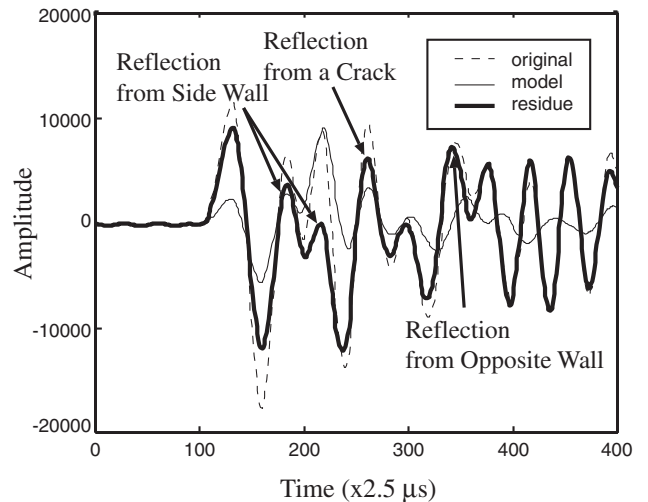


Fig. 8 Original output, the modeled output of the surface wave, and their residue using the previously proposed method.

- (2) The response is expressed by Eq. (1). Therefore, the absolute values of the peaks should decrease as time passes. If the absolute value of the i th peak is larger than that of the $(i - 1)$ th peak, a reflection exists between the $(i - 1)$ th peak and the i th peak. For this reason, the end of the duration is set at the zero-cross point after the $(i - 1)$ th peak.

Figure 9 shows that a large fraction of the surface wave is eliminated compared with Fig. 8. Moreover, peaks caused by reflections from the crack and side walls clearly

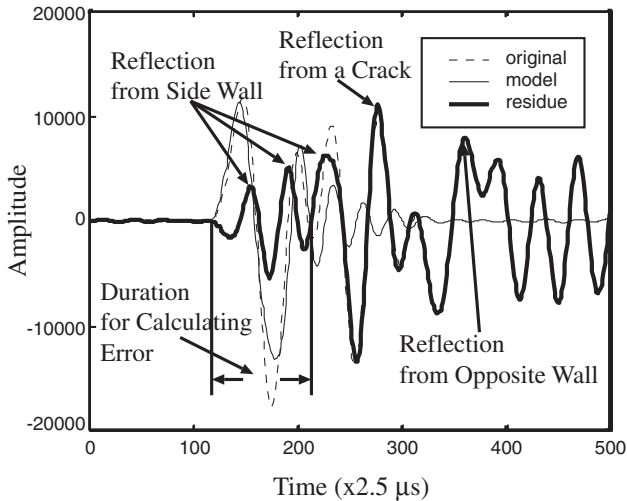


Fig. 9 Original output, the modeled output of the surface wave, and their residue using the proposed method.

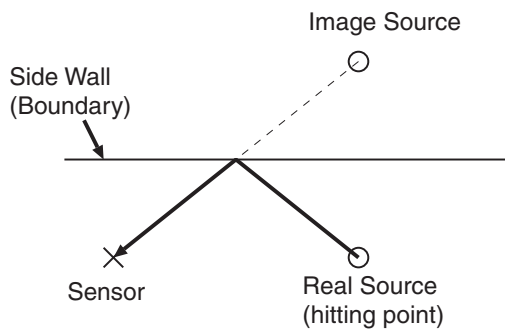


Fig. 10 Hitting point (real source) and its image source due to the mirror effect.

appear in the residual, because the reflection from side walls remains unchanged by the new method. Because we wish to know the position of the crack, the reflection from the side wall is interference or noise that should be eliminated; the reflection from the crack or opposite wall is the “desired” signal.

If the shape of the concrete structure is known, an image source can be assumed because of the mirror effect, as shown in Fig. 10, and the propagation distance from the hitting point to the sensor is calculated. In Figs. 8 and 9, some peaks are marked with “reflection from side wall” because their positions coincide with the positions attributable to the reflections from the side walls, as calculated from the propagation distance and the surface-wave velocity. On the other hand, another peak is marked with “reflection from a crack” because its position coincides with the position attributable to the reflection from a crack, which is calculated from the propagation distance and the velocity of the primary wave.

Because the peaks that are attributable to the reflective waves from the side walls and the crack appear clearly in

the residue, the positions of the side walls and the crack can be estimated by applying the near-field beamforming technique [7] to the residue.

3. NEAR-FIELD BEAMFORMING

The positions of the point of impact and the accelerometers are known, and the primary-wave velocity can be estimated by the positions of the peaks in the accelerometer output. Therefore, the crack position is estimated using near-field beamforming [5–7].

In this method, an imaginary source is assumed first. Then, under the free-field assumption, the distances between the imaginary source and all the accelerometers are calculated. All accelerometer outputs are shifted in the time domain to compensate the propagation delay. Then, the compensated signals are averaged. If the number of accelerometers is P and the peak positions of the compensated signals are random, the peak value of the average compensated signal decreases in inverse proportion to \sqrt{P} in cases where the position of the imaginary source does not coincide with that of a real source. Otherwise, it remains unchanged. The position of the imaginary source is scanned in the space to be investigated. The estimated position of the real source is the position at which the value of the averaged signal yields a large peak.

Because the time of impact and the velocities for the three propagation modes are known, the time at which the reflection from the crack appears in the accelerometer output can be estimated. To improve the SNR, each accelerometer output was cut out with a time window so that the time-window position is the position reached by the reflection from the crack. The time-window shape is identical to that obtained by the output of the impulse hammer. Here, the maximum difference in the distance between the crack and each accelerometer was about 1 m in the experiment, which corresponds to about 0.25 ms time difference, since the velocity of the primary wave is about 4,000 m/s. On the other hand, the duration of the waveform caused by the impact force is also about 0.25 ms, as shown in Fig. 2. Thus, the positions of the peaks due to the reflection from the crack overlap each other. Furthermore, the hitting point is near the accelerometer array, and the directivity pattern obtained by such a small accelerometer array is not sharp. Therefore, a circular pattern was observed, where the radius of the circle is nearly equal to the distance between the hitting point and the crack [6]. Only the peaks directly below the hitting point are authentic because the pattern is circular, and the primary wave is dominant for the reflection from a crack directly below the point of impact.

4. EXPERIMENT

Six equispaced accelerometers and three concrete

species with a size of 1.2 m × 1.2 m × 0.3 m, as shown in Fig. 7, were used for this experiment. We used only six accelerometers because of the cost; only about 8 dB of SNR improvement is expected.

The first species (a) has no crack, the second (b) has a parallel crack, and the third one (c) has a slanted crack. The crack was made by burying a sheet of 1-cm-thick plywood. The sizes of the cracks are 0.8 m × 0.3 m × 0.01 m for the parallel crack (b), and 0.9 m × 0.3 m × 0.01 m for the slanted crack (c). The crack sizes used in the work by Harayama *et al.* [8] were $\phi 175 \times t50$ mm and $\phi 350 \times t50$ mm, which were, respectively, about one-quarter or half the width and five times thicker than the cracks shown in Fig. 7. The crack size was 3.0 m × 1.5 m × 0.2 m in the work by Sansalone and Carino [3], which was about four times wider and 20 times larger in thickness than the cracks shown in Fig. 7. Therefore, the crack size used in our experiment seems plausible, since the wavelength of the signal used in our experiment is almost the same as those in the above studies [3,8]. The velocity was 3,800 m/s for the primary wave, which was estimated using the positions of the peaks in the outputs of the accelerometers. The position of the *i*th accelerometer is $(x, y, z) = (0.075 + 0.15i \text{ m}, 0.0 \text{ m}, 0.15 \text{ m})$, and the hitting point is $(x, y, z) = (0.6 \text{ m}, 0.0 \text{ m}, 0.15 \text{ m})$ in Fig. 7.

First, we examined the method using the resonant frequency [3]. Let *d* be the distance between the surface plane and the sheetlike crack plane. Then, the relation $d = \lambda/2$ is established, where λ is the wavelength of the lowest-resonant-frequency component [3]. The surface wave was not eliminated in this method. Figure 11 shows the power spectrum of an accelerometer output in the case of one parallel crack shown in Fig. 7(b). In this case, because the hitting surface and the crack surface are parallel, large peaks should be observed only at the resonant frequencies of the standing waves. However, many peaks are observed at frequencies that are not

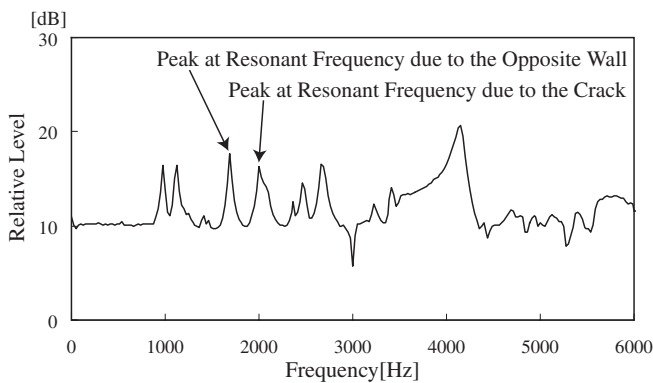


Fig. 11 Power spectrum of an accelerometer output for the concrete structure with a single parallel crack shown in Fig. 7(b).

resonant frequencies. They are caused by the numerous reflections from the boundaries of the concrete structure. Consequently, it is difficult to estimate the crack position. The peak caused by the standing wave was not dominant, probably because (1) a standing wave also occurs between side walls, and (2) the significant surface wave was not eliminated. The crack might be detected by comparison to the peaks of a structure without any crack. However, an identical structure with no crack cannot always be supplied if it is very large. Furthermore, if a crack exists deep within the structure, the reflection wave power is small and a standing wave might not be generated. In such cases, the method of detecting a crack by comparison is difficult.

Figures 12–17 show the results of near-field beamforming, which gives the values of the averaged powers of peaks, as illustrated by contour lines.

Figure 12 shows the result for the concrete structure (a) without any crack. It was obtained using the previously proposed method [6], which eliminated the influence of both surface-wave and side-wall reflections. A large peak (97 dB) is observed at the opposite position to the point of impact, because the primary wave reflected from the opposite side (1.2 m) has a large amplitude. Nevertheless, a large peak (94 dB) is apparent at 0.8 m depth inside the structure, which appears because the suppression of the reflection from the side wall was insufficient. Its power is less than the peak at 1.2 m by about 3 dB.

The primary wave is well known to be dominant for the reflection from a crack directly below the point of impact. In circular patterns whose respective radii are 1.2 m and 0.8 m, the *x* values of the largest peaks are almost equivalent to that of the point of impact ($x = 0.6 \text{ m}$). On the other hand, in circular patterns with a radius of 1.0 m, the *x* value of the largest peak is 1.3 m, and the value at

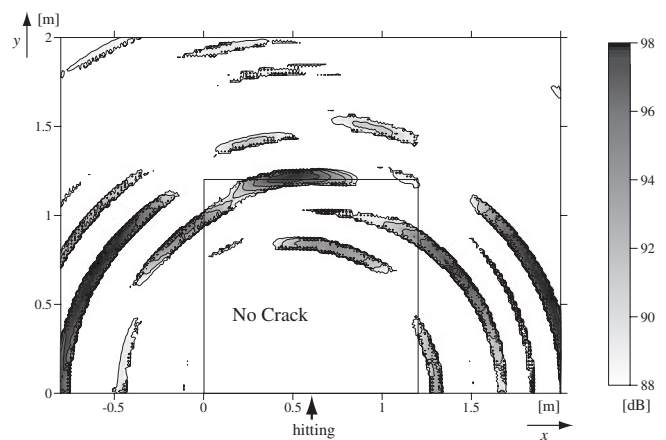


Fig. 12 Result of the near-field beamforming using the previously proposed method for the concrete species with no crack shown in Fig. 7(a).

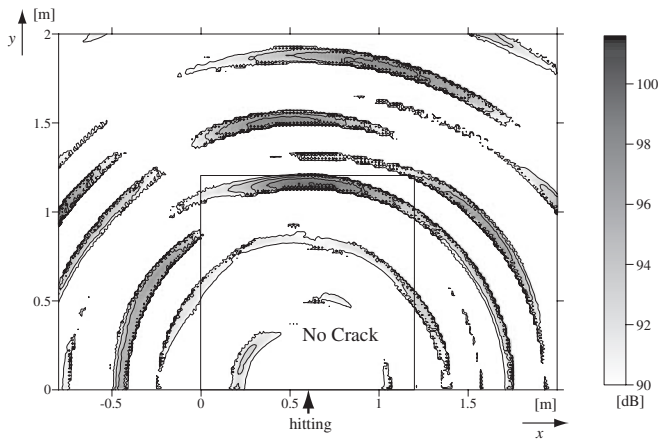


Fig. 13 Result of the near-field beamforming using the newly proposed method for the concrete species with no crack shown in Fig. 7(a).

$x = 0.6$ m is small. For that reason, we can infer that no crack exists near $(x, y) = (0.6$ m, 1.0 m).

Figure 13 shows the result obtained using the newly proposed method for the same case. Similarly, the largest peak (97 dB) is observed at the opposite side (1.2 m). In the circular patterns whose radii are 0.4 m and 0.8 m, the x values of the largest peak are not near the x value of the impact point, and the values at $x = 0.6$ m are small. Therefore, we can infer that the circular patterns might not be the result of a crack. As described in Sect. 2.2, the circular pattern (93 dB) (radius: ca. 0.4 m) is attributable to the reflection from the side wall, which remains unchanged because the new method does not eliminate this reflection, although it is eliminated by the previous method, as shown in Fig. 12. A circular pattern (92 dB) (radius: ca. 0.8 m), which arises because of the multiple reflection from the side wall, is observed. The value of the pattern is, however, smaller by 2 dB than that obtained using the previous method, because the elimination of the reflection from the side wall by the previous method is insufficient. The previous method sometimes increases the value of the peak because of a reflection from the side wall. The elimination performance seems to weaken or worsen for longer distances between the hitting point and the reflection point.

Because the shape of the concrete structure is known, the arrival time of the reflection from the side wall is calculable and the radii of the circular pattern can be evaluated. Therefore, if a circular pattern is observed at the position where the pattern caused by reflection from the side wall does not appear, that pattern is caused by a crack.

Figure 14 shows the result obtained using the previously proposed method for the case of the concrete structure (b) with a parallel crack. A large peak (81 dB) is visible near the opposite side (depth: 1.2 m). Another large peak (83 dB) is apparent near the crack position

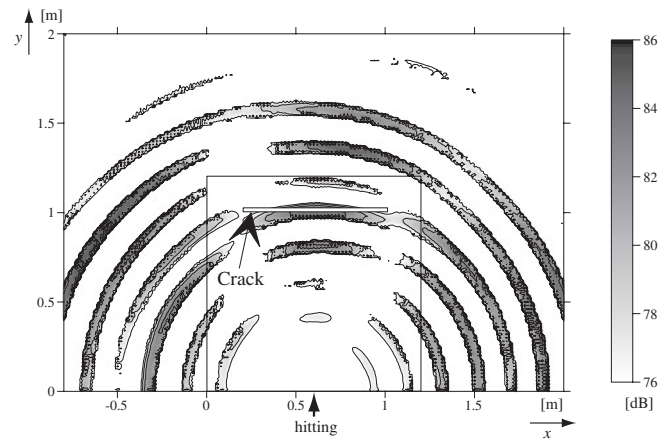


Fig. 14 Result of the near-field beamforming using the previously proposed method for the concrete species with a parallel crack shown in Fig. 7(b).

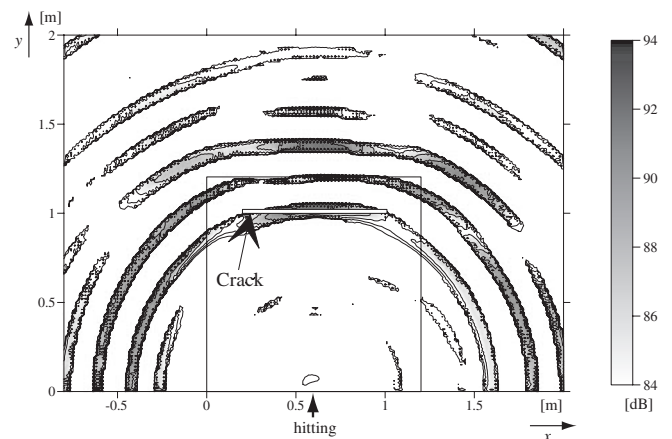


Fig. 15 Result of the near-field beamforming using the newly proposed method for the concrete species with a parallel crack shown in Fig. 7(b).

(depth: 1 m), but a large peak (82 dB) is also visible directly below the crack (depth: 0.8 m). It is difficult to estimate the actual crack position from Fig. 14. The values of the peaks at the opposite side and at the crack are smaller than the peak (depth: 0.8 m) because of the reflection from the side wall resulting from its non elimination. That is, the previous method might not only suppress the reflections from the side walls, it might also suppress the peaks due to the crack and the opposite side.

Figure 15 shows the result obtained using the newly proposed method for the same case. A large peak (92 dB) inside the concrete structure appears at the opposite wall ($y = 1.2$ m). A large peak (91 dB) inside the concrete structure appears at the crack ($y = 1.0$ m). Other peaks inside the structure are generated because of the reflections from side walls, as in Fig. 13. The value of the peak attributable to the side wall is about 86 dB, which is smaller

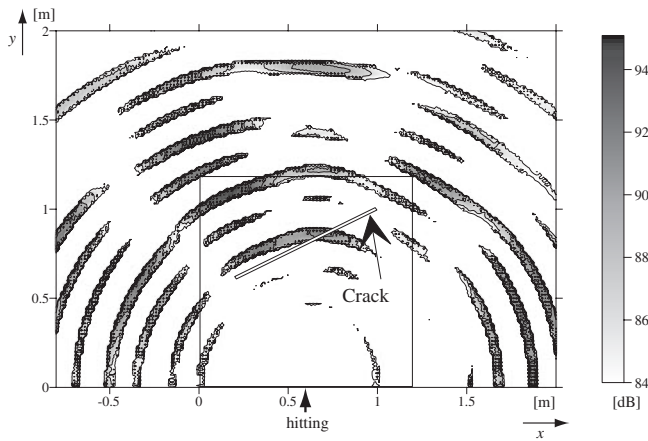


Fig. 16 Result of the near-field beamforming using the previously proposed method for the concrete species with a slanted crack shown in Fig. 7(c).

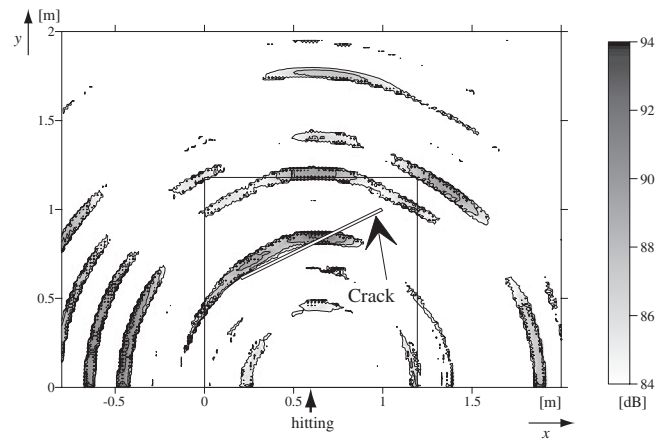


Fig. 17 Result of the near-field beamforming using the newly proposed method for the concrete species with a slanted crack shown in Fig. 7(c).

than that caused by the crack or the opposite wall by about 5 dB. This value is the same as that in the case of the concrete structure (a) with no crack shown in Fig. 13.

The primary wave is dominant for a reflection from a crack directly underneath the point of impact. If a crack exists directly underneath the impact point, the largest peak in a circular pattern will be observed directly underneath the impact point, although the value directly underneath the impact point will be small if no crack exists there. Therefore, the crack size might be roughly evaluated by changing the impact point.

Figures 16 and 17 respectively show the results obtained using the previously proposed method and the newly proposed method for the case of the concrete structure (c) with a slanted crack. The technique using the resonant frequency does not work well theoretically in this case. In Fig. 16, a large peak (about 91 dB) is observed at the opposite side (depth: 1.2 m), and another large peak (about 92 dB) is observed along the slanted crack. However, other peaks (ca. 86–92 dB) are visible inside the structure. The peak (86 dB) around $(x, y) = (1.0 \text{ m}, 0.0 \text{ m})$ might be attributable to the reflection waves from the side walls ($z = 0 \text{ m}$ and 0.3 m). The peak (91 dB) around $(x, y) = (0.2 \text{ m}, 0.8 \text{ m})$ might be caused by the surface waves, where the value of the peak increases because of their non elimination.

On the other hand, in Fig. 17, two large peaks with almost equal values as those in Fig. 16 are observed at the opposite wall and the crack. However, no peak, except for that caused by the reflection from the side wall, is observed in Fig. 17, and the value of the peak caused by the side wall is about 86 dB, which is smaller than that caused by the crack or the opposite wall by about 5 dB. This value is the same as that in the cases of the concrete structures (a) and (b).

In Figs. 13, 15, and 17, which show results obtained using the new method, the peak value attributable to the reflections from side walls ($z = 0.0 \text{ m}$ and 0.3 m) is about 5 dB smaller than that caused by the opposite wall (1.2 m), although the peak value caused by the crack is almost equal to that caused by the opposite wall. Therefore, it is easy to detect the crack position from the figures. That is, if a peak is apparent at the position where a peak resulting from the reflection from the side wall might appear, and the value of the peak is almost equal to that of the largest peak, it indicates a crack. The new method cannot detect a crack position, however, if the pattern resulting from a crack overlaps with that caused by a side wall and if the size of the crack is small so that the amplitude of the reflection from the crack is small. To detect such a crack, the extraction of the exact reflection wave from the side wall is required, but this is difficult because the reflection-wave shape does not resemble that of the direct wave. A method for extracting the exact reflection wave remains a subject for future work.

5. CONCLUSION

In this paper, we described a new method, using several accelerometers, to improve the crack detection performance for a concrete structure. We compared three methods: (1) the conventional method [3] using the resonant frequency, (2) the previously proposed method [6], and (3) a new method for estimating the surface wave more precisely. Results show that the first method did not work well in two cases: (1) when the crack surface is not parallel to the structure surface, and (2) when the concrete structure is a small rectangular parallelepiped, in which case two or more resonant frequencies might appear. The second and the third methods described above, using the first reflection wave from the crack instead of the resonant frequency,

detected cracks in both of the above-mentioned cases. Nevertheless, the second method showed several peaks at positions where no crack existed because estimation of the surface wave was insufficiently accurate. That is, the second method might not only suppress the reflections from the side walls: it might also suppress the peaks due to the crack and the opposite side. The third method proposed in this paper was able to suppress the peaks due to the surface wave, but it did not suppress the peaks due to the crack and the opposite side, thereby facilitating clearer observation of the crack. This result demonstrates the effectiveness of the new method.

ACKNOWLEDGMENTS

The authors are deeply indebted to Mr. Taniguchi and Mr. Takahashi of Tokyo Soil Research Co., Ltd. for providing us with the concrete structures for experiments.

REFERENCES

- [1] K. Preiss, "Checking of cast in place concrete piles by nuclear radiation methods," *Br. J. Non-Destr. Test.*, **13**, 70–76 (1971).
- [2] J. K. C. Shih, R. Delpak, C. W. Hu, D. B. Tann and D. B. Moore, "The use of IR thermography in structural health monitoring," *Struct. Health Monit. Intell. Infrastruct.*, **2**, 687–692 (2003).
- [3] M. Sansalone and N. J. Carino, "Detecting delaminations in concrete slabs with and without overlays using the impact echo methods," *ACI Mater. J.*, **86-M18**, 175–184 (1989).
- [4] K. Kaito, M. Abe, Y. Fujino and K. Kumasaka, "Detection of internal voids in concrete structures using local vibration information," *J. Mater. Concrete Struct. Pavements*, **690/V-53**, 121–132 (2001).
- [5] M. Abe, S. Hongo, Y. Nemoto and Y. Chubachi, "Non-destructive technique to estimate the position of a crack in a concrete block buried in the ground," *Proc. 3rd Int. Congr. Air- and Structure-Borne Sound and Vibration*, Vol. 3, 2045–2052 (1994).
- [6] M. Abe, T. Fujioka and Y. Nagata, "Location of a defect in a concrete block by a non-destructive technique," *Acoust. Sci. & Tech.*, **23**, 308–312 (2002).
- [7] M. Abe, Y. Nagata and K. Kido, "A new method to locate vibration sources by searching the minimum value of error function," *Proc. IEEE Int. Conf. Acoust. Speech Signal Process.*, 18B.2.1–2.4 (1986).
- [8] Y. Harayama, M. Nihei, H. Takenouchi, M. Enokizono and N. Takemoto, "Development of a continuous impact sound inspection system for concrete structures," *Struct. Health Monit. Intell. Infrastruct.*, **2**, 673–682 (2003).



Takeshi Murakami was born in Aomori, Japan, on November 26, 1973. He received B.E. and M.E. degrees from the Department of Computer and Information Science, Faculty of Engineering, Iwate University in 1995 and 1997, respectively. His research interests include non-destructive measurement and signal processing.



Toyota Fujioka received the B.E. and M.E. in Electrical and Electronic Engineering from the Mining College, Akita University in 1992 and 1994, respectively, and the Ph.D. in Electrical and Communication Engineering from Tohoku University in 1997. He is currently a Research Associate of the Department of Computer and Information Science Faculty of Engineering, Iwate University. His research interests include digital signal processing for acoustics and computer architecture. He is a member of the Information Processing Society of Japan and the Institute of Electronics, Information and Communication Engineers.



Yoshifumi Nagata received the B.E. degree in Electronics in 1984, M.E. and Dr. Eng. degrees in information science in 1987 and 1990 respectively all from Tohoku University, Sendai, Japan. In 1990, he joined Research and Development Center, Toshiba Corporation, where he has been engaged in research and development of speech processing systems. From 1997, he is an associate professor at the Iwate University, Morioka Japan. His interests include multimedia human interface and speech signal processing. He is a member of Acoustical Society of Japan, Information Processing Society of Japan.



Masato Abe received the B.E., M.E. and Ph.D degrees in electrical engineering from the Tohoku university in 1976, 1978 and 1981, respectively. From 1981 to 1989 he was at Research Center for Applied Information Sciences, Tohoku University as a research associate. From 1989 to 1996 he was an associate Professor at Computer Center, Tohoku University. He is now a professor at Department of Information Science, Iwate University, Japan. His research interests include digital signal processing for acoustics and computer architecture. He is a member of IEEE, Acoustical Society of America, Acoustical Society of Japan, the Institute of Noise Control Engineering of Japan, Information Processing Society of Japan, the Institute of Electronics, Information and Communication Engineers, Association for Computing Machinery, and the Japan Society of Mechanical Engineers.